Optical design of ARIES: the new near infrared science instrument for the adaptive f/15 Multiple Mirror Telescope

Roland J. Sarlot[a], Donald W. McCarthy[a], James H. Burge[ab], Jian Ge[c]

[a]Steward Observatory, University of Arizona, Tucson, AZ, 85721, USA
[b]Optical Sciences Center, University of Arizona, Tucson, AZ, 85721, USA
[c]Lawrence Livermore National Laboratory, Livermore, CA, 94551, USA

ABSTRACT

Steward Observatory is building a deformable f/15 secondary mirror that will compensate for atmospheric turbulence for the 6.5 m Multiple Mirror Telescope conversion. With the proposed adaptive optics system, this new telescope is expected to resolve diffraction limited images (greater than 80% Strehl ratio at 2.2 μm), approximately an order of magnitude better than present seeing. This improved visibility with a larger light collecting area and low thermal background requires a new science instrument, diffraction limited for the 1 to 5 μm region. This science instrument, presently in its early manufacturing stages, consists of four cameras (optimized for plate scales from 0.019 arcsec/pixel to 0.102 arcsec/pixel), low resolution spectroscopy with grisms ($\lambda/\Delta\lambda$ from 250 to 500), high resolution spectroscopy with a cross-dispersed Echelle grating ($\lambda/\Delta\lambda$ from 3,000 to 60,000) and an atmospheric dispersion corrector. The cameras will provide simultaneous slit viewing, differential imaging and two pixel sampling over the full wavelength band. Each camera will operate with a 1024x1024 HgCdTe array optimized for the spectral region of the camera. An infrared tip/tilt sensor is also incorporated into the instrument that will relay natural guide star motion to the adaptive secondary in a closed-loop approach. This paper is an optical design instrument overview.

Keywords: adaptive optics, infrared, camera, spectrograph, atmospheric dispersion corrector, MMT

1. INSTRUMENT DRIVERS

The design of the Arizona Infrared Imager and Echelle Spectrograph (ARIES) was driven by several factors based on three independent technical advances. The primary driver was to take full advantage of the telescope upgrade. In particular, the monolithic 6.5 m Multiple Mirror Telescope (MMT) primary's upgrade light gathering capability and the new adaptive secondary mirror which is actively controlled in real time to compensate for atmospheric turbulence[1]. Both mirrors and a 10% best seeing night are expected to resolve images with a Strehl ratio greater than 80% on-axis at 2.2 μm[2]. An additional advantage of the deformable secondary mirror is that no additional relay optics are necessary for atmospheric compensation. The only ambient temperature surfaces are the primary and secondary telescope mirrors and the dewar window guaranteeing low thermal background. All other surfaces are within the dewar and cooled to 77 Kelvin[3].

An additional design goal was to incorporate the advances in detector technology. Infrared focal plane arrays have improved dramatically over the last few years in detector area as well as having lower readout noise, wider spectral sensitivity and quantum efficiencies greater than 60%.

The third instrument driver for the design of ARIES is to satisfy the scientific needs of a broad community interested in capitalizing on the unique advantages of the MMT's adaptive optics (AO) system. This system allows ARIES to provide efficient diffraction-limited imaging at all wavelengths from 1-5 microns as well as nearly three decades of spectroscopic resolution (100-60,000) in a relatively compact instrument. The ability to perform simultaneous imaging and/or spectroscopy in two wavebands will help calibrate the point spread function of the AO system.

These capabilities will be especially powerful in the thermal-infrared (>2.5 microns) where the adaptive secondary mirror allows low background operation and where numerous molecular transitions become available for examining the physical and chemical characteristics of stellar and planetary atmospheres, including some of the recently discovered brown dwarfs and extra-solar planets.

Part of the SPIE Conference on Current Developments in Optical Design and Optical Engineering VIII • Denver, Colorado • July 1999
SPIE Vol. 3779 • 0277-786X/99/$10.00

2. DETECTORS

Three HgCdTe detectors are incorporated in ARIES. Two 1024x1024 pixel arrays are used for science observations in two independent wavebands from 1-2.5 and 1-5 microns. The latter will use Rockwell's new molecular beam epitaxy (MBE) array operating at ~50 K; the former uses Rockwell's HAWAII array. These two detectors can be operated simultaneously to provide efficient imaging of objects over a wide bandpass, a slit viewing/guiding capability, and calibration observations for the system.

The third detector, not yet specified, provides rapid centroid measurements of a random field star to the AO system for correcting the tip/tilt component of the wavefront. At first light, this tip/tilt detector will likely utilize a small (~4x4 pixel) subarray of a HAWAII array (~10 electron read noise). Later we hope to use a HgCdTe array on Rockwell's TCM-2727 multiplexer to obtain read noise ~1-2 electrons.

3. CHOICE OF FOCAL LENGTHS

The focal lengths of the various cameras were chosen to provide two pixel sampling (λ/2D) of the Nyquist limit for both science arrays over the five atmospheric bands between 1 and 5 μm. For a wavelength of 1.25 μm, this corresponds to 0.0198 arc second pixels and sampling the diffraction limit at 2.2 μm corresponds to 0.0349 arc second pixels. Figure 1 illustrates the instrument's imaging regions. The f/5.6 imaging camera was designed to survey the sky over a wide field and was not designed to be diffraction limited. Table 1 lists the first order specifications for each of the optical channels.

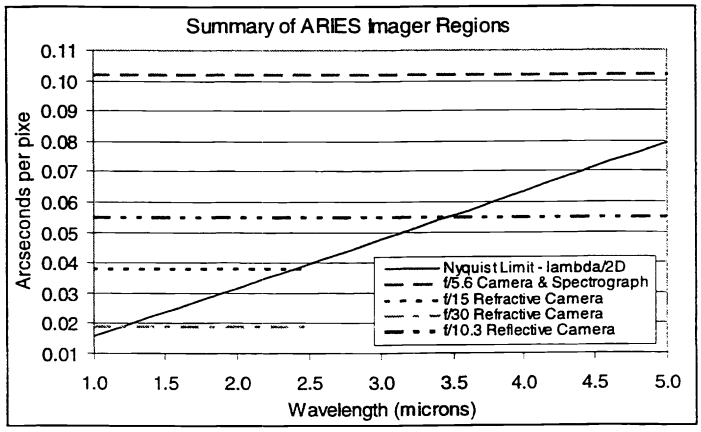

Figure 1. Summary of imager regions. The graph represents the two pixel Nyquist sampling limit and the angular resolution of each camera over the 1 to 5 μm spectral region. The f/5.6 camera was not designed for diffraction limited images, but rather, for a wide field.

	Slit View Camera	Slit View Camera	Reflective Spectrograph and Camera	LM Band Imager	Tip/Tilt Detector
Detector	HgCdTe	HgCdTe	HgCdTe	HgCdTe	HgCdTe
Pixels across detector	1024 x 1024	1024 x 1024	1024 x 1024	1024 x 1024	128 x 128
Pixel size	18.5 μm	18.5 μm	18.5 μm	18.5 μm	40 μm
Wavelength	1.1 – 2.5 μm	1.1 – 2.5 μm	1.0 – 5.0 μm	2.5 – 5.0 μm	1.1 – 2.0 μm
Focal ratio	f/15	f/30	f/5.6	f/10.3	f/8.46
Plate scale	2.11 arcsec/mm	1.06 arcsec/mm	5.67 arcsec/mm	3.08 arcsec/mm	3.75 arcsec/mm
Field per pixel	0.038 arcsec/pixel	0.019 arcsec/pixel	0.102 arcsec/pixel	0.055 arcsec/pixel	0.15 arcsec/pixel
Full field (inscribed on detector)	40.0 arcseconds	20.0 arcseconds	104.4 arcseconds	56.8 arcseconds	2.4 arcminutes

Table 1. Summary of cameras' specifications. The first order design requirements for each of the four cameras including the tip/tilt sensor are described. Note that the full field diameter is not imaged onto the tip/tilt detector, but rather, the detector is steered manually through this field.

4. OPTICAL DESIGN

The four cameras of the science instrument are best methodologically divided into seven optical subsystems. The components are, in the direction of incoming light, the dichroic window, AO tip/tilt sensor, the Offner relay, the atmospheric dispersion corrector, the short wavelength cameras, the refractive collimator and gratings, and the long wavelength cameras. The subsystems through the atmospheric dispersion corrector will be utilized for all configurations. Figure 2 is a layout of the full optical system.

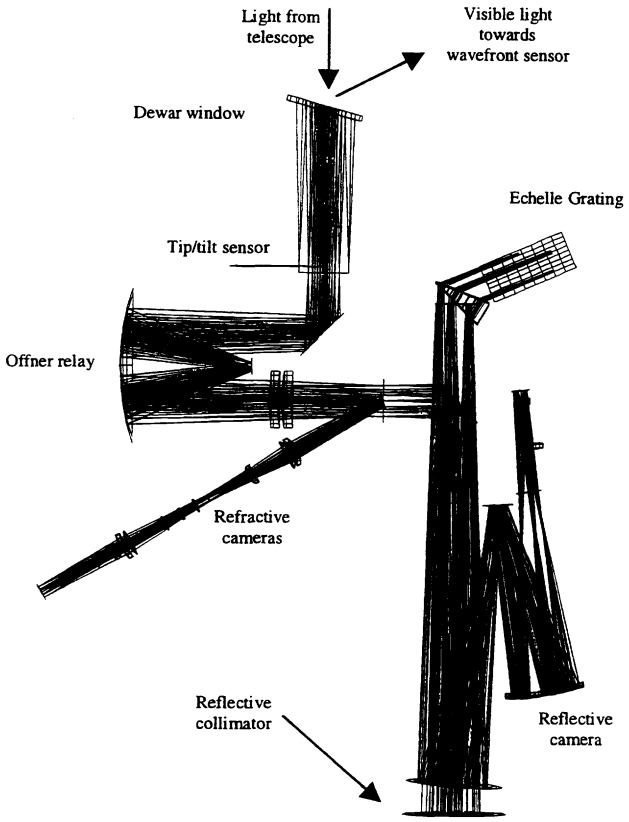

Figure 2. Full layout of optical design. The entire optical design is displayed from the dichroic window through both detectors, the tip/tilt sensor and the high resolution cross dispersed Echelle spectrograph. The other two spectrographs are not illustrated here. The three mirror reflective camera is out of the plane of the paper.

4.1. Dichroic window

Mechanically, the dichroic window serves as the vacuum seal to the dewar and should be strong enough to protect the instrument from any reasonable physical shock. The window will be mounted at 15° from the incident light in a bellows attachment so that the reflection from the front surface can be adjusted in tip/tilt and focus to feed the visible science instruments and the laser guide star wavefront sensor. Optically, the window will highly transmit the infrared region of interest and reflect visible light from 0.35μm to 1.0μm with a peak reflectance at 589nm, the wavelength of the sodium guide star. The average nominal reflectivity approximates 95% with transmission around 98%.

The proposed dewar window substrate is a plano/plano 120 mm diameter, 8 mm thick crystal of calcium fluoride coated with an interference filter on the exterior surface of the dewar. The inside surface will be coated with a anti-reflection coating to increase the transmission approximately 1.5%. Safety analysis performed on the window with the maximum stress equal to ¼ the elastic limit, an appropriate safety factor for dewar applications. The vacuum analysis indicated a sag from flat of 38.5 μm. with an rms wavefront error of 0.019 waves at 1.25μm.

4.2. Adaptive optic tip/tilt sensor

The basic premise of the optical design is to reflect a small portion of the Cassegrain image by placing a reflective fold flat 10 mm before the Cassegrain image plane. This image is then redirected, collimated and directed onto imaging optics in front of

the detector. The collimated space allows for a variable spacing between the lenses and allows the mechanical probe to extend over the two dimensional field without disturbing the image quality.

Figure 3 is the layout of the optical design. The detector will use a quad cell approach to track lateral object motion. The probe will be steered through the wide field by viewing the probe shadow on the two main science detectors. The Cassegrain focus remains unobscured and future instrument upgrades may implement coronograph capabilities.

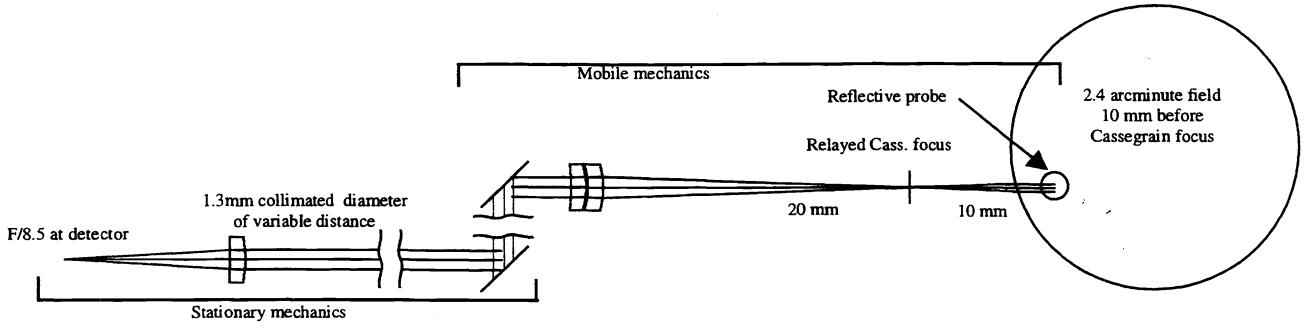

Figure 3 Global tip/tilt sensing optics. A small reflective probe is inserted into f/15 telescope beam to redirect light towards the quad detector and sense global tip/tilt of the science object. The collimated light is of variable length and allows the reflective probe relayed image to be in focus for any position over the Cassegrain focus. Values illustrated are paraxial.

4.3. Offner relay

The design utilizes an Offner relay to reimage the wide-field Cassegrain focus to a more convenient location as well as provide a "cold" pupil for thermal baffling. The intermediary pupil, located at the secondary mirror, will be defined by a 12.80 diameter hole in a black surface and serve as the entire system stop thereby vignetting stray thermal radiation from the edge of the telescope secondary mirror. The relay additionally allows an unrestricted image plane for the infrared tip/tilt sensing device with a variety of options at the relayed image plane such as reflective slits, dichroic plates and mirrors. Figure 4 is a side view of the two spherical mirrors relaying the image plane. The pupil mask will be checked for alignment with the secondary telescope mirror with pupil viewing optics explained later.

The Offner mirrors, as all mirrors in the instrument, will be manufactured from fused silica. Although the coefficient of thermal expansion of this material will not match the aluminum dewar material, we traded ease of alignment over a large temperature change with lower scatter and better surface figure.

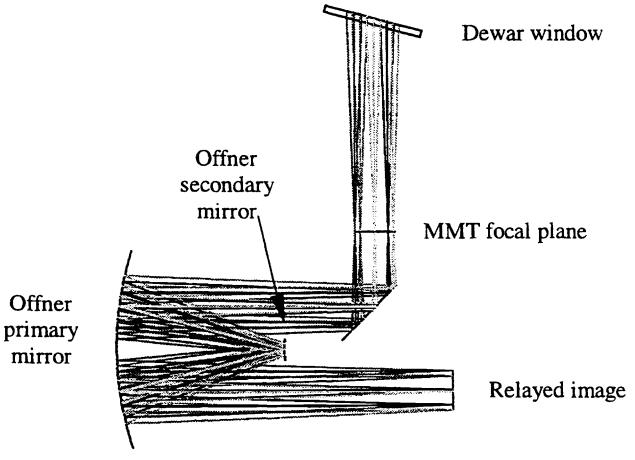

Figure 4. Dewar window and Offner relay. The fore optics channel of ARIES consists of a dichroic dewar window, transmitting the infrared and reflecting the visible towards the wavefront sensor and visible science cameras. Focusing 250 mm past the dewar window is the 50.7 mm diameter Cassegrain image plane of the telescope which is then relayed by the 1-to-1 Offner two mirror relay.

4.4. Atmospheric dispersion corrector

At 45° from zenith, the effects of atmospheric dispersion will elongate the image beyond the Airy disk diameter with lateral color by a factor of 2.3 at 2.2 μm for the edge of the tip/tilt field. The converging rays of the Offner relay will contain an atmospheric dispersion corrector (ADC) to compensate for this effect. The design concept uses two sets of prisms with curved surfaces, countering rotating with respect to each other as a function of zenith angle, inducing first order lateral dispersion opposite to that of the atmosphere[4]. A close-up illustration of the lenses as well as their location in the Offner converging beam is depicted in Figure 5.

The goal of the ADC was to correct images over the widest field, to 60° from zenith over the full 1 to 5 μm spectral band to better than 0.1 arcseconds, the best seeing slit width. The prisms must compensate not only for atmospheric effects but also for instrument rotation, color induced by the dewar window and be used for all imaging and spectroscopy modes. In early design phases, it was not established whether the ADC would be implemented in the first manufacturing phase, so the ADC was designed with curved surfaces to not offset the focal plane position due to the additional material[5]. Although the ADC is now considered an integral component of the system and will be implemented in the first version of the instrument, the zero power of the curved surfaces will be kept in the design so that if any mechanical rotational failures occur, the lenses can be manually removed from the incoming light and the instrument can continue operating.

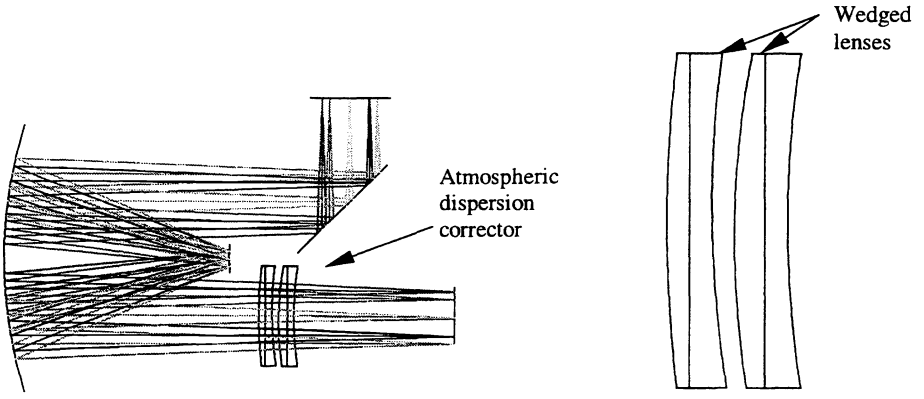

Figure 5. Atmospheric dispersion corrector. The figure on the left shows the ADC within the converging Offner beams. The figure on the right is a magnified image of the four CaF2 and LiF lenses. Each doublet pair is air spaced, identical and counter-rotating. The two inner lenses have an induced wedge angle of 0.888°.

4.5. Short wavelength channel

The objectives of the short wavelength channel are to image and perform low resolution spectroscopy with grisms over the J, H and K atmospheric windows. The focal lengths were chosen to provide two pixel Nyquist sampling at the diffraction limit (λ/2D) and the cameras were designed to provide diffraction limited viewing over 40 arcseconds. Additional goals of these cameras were to provide imaging for guide star acquisition, slit viewing and differential imaging.

	Slit View Camera	Slit View Camera
Detector	HgCdTe	HgCdTe
Pixels across detector	1024 x 1024	1024 x 1024
Pixel size	18.5 μm	18.5 μm
Wavelength	1.1 – 2.5 μm	1.1 – 2.5 μm
Focal ratio	f/15	f/30
Plate scale	2.11 arcsec/mm	1.06 arcsec/mm
Field per pixel	0.038 arcsec/pixel	0.019 arcsec/pixel
Full field (inscribed on detector)	40.0 arcseconds	20.0 arcseconds

Table 2. Refractive camera parameters. Listed are the first order design requirements for each of the two short wavelength channel cameras.

These cameras are fed by a reflective surface at the relayed Offner image plane, tilted at 15 degrees from the incoming beam. The optics for this channel include one refractive collimator with two sets of interchangeable camera lenses for imaging at

f/15 and f/30 with a constant overall length for both cameras to share a common detector. Figure 6 illustrates the various refractive cameras. This channel can additionally be utilized for imaging during real-time spectroscopy and the excellent pupil in collimated space allows for low resolution 1.0 – 2.5 μm spectroscopy with grisms. All lenses are manufactured from BaF2 and SF6 and have spherical surfaces. The short wavelength channel detector is a Rockwell HgCdTe sensitive between 1 and 2.5 μm. We are presently defining grism specifications.

The short wavelength channel also incorporates a pupil viewing mode whereby a third set of lenses can rotate into the same position as the refractive cameras and image the secondary telescope mirror and the secondary Offner mirror, both system pupils, simultaneously. Imaging in this mode will allow the alignment of the pupils so that the Offner secondary mirror will properly baffle the larger mirror for thermal radiation reduction. Imaging will be at 1.25 μm with two BaF2 lenses, one spherical, the other cylindrical.

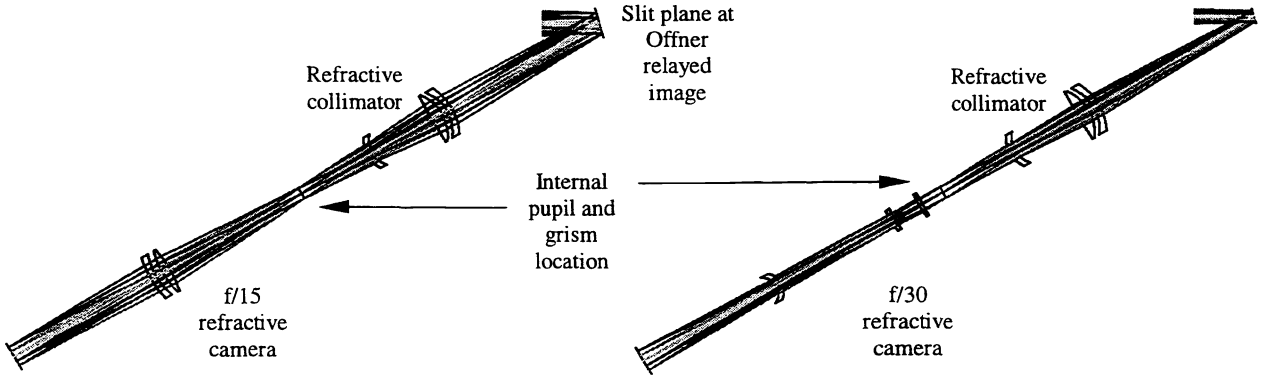

Figure 6. Refractive cameras. The first three lenses of the short channel (at the upper right of each figure) reimages the intermediate focal plane from the Offner relay through a collimated pupil and onto the HgCdTe detector at the left of each figure. The two lens camera on the left images at f/15, on the right for the f/30 camera. In addition, another set of lenses is rotated into the camera position for pupil imaging.

4.6. Long wavelength Channel

The long wavelength channel is defined as the reflective path after the Offner relay that images and performs spectroscopy over the 1 to 5 μm spectral band. Goals of this component were to provide two focal ratios, direct imaging, three spectroscopy modes and diffraction limited imaging over 56 arcseconds.

	Reflective Spectrograph and Camera	LM Band Imager
Detector	HgCdTe	HgCdTe
Pixels across detector	1024 x 1024	1024 x 1024
Pixel size	18.5 μm	18.5 μm
Wavelength	1.0 – 5.0 μm	2.5 – 5.0 μm
Focal ratio	f/5.6	f/10.3
Plate scale	5.67 arcsec/mm	3.08 arcsec/mm
Field per pixel	0.102 arcsec/pixel	0.055 arcsec/pixel
Full field (inscribed on detector)	104.4 arcseconds	56.8 arcseconds

Table 3. Reflective camera parameters. Listed are the first order design requirements for each of the two long wavelength channel cameras.

The long wavelength channel consists of an off-axis parabola collimating the light from the slit plane and reimaging the object at infinity with a three mirror anastigmat. This all reflective system images at an f/5.6 focal ratio. Inserting two lenses before the focal plane changes the focal ratio to f/10.3. Figure 7 shows the three mirror anastigmat[6] with a pupil out front and imaging light from infinity to a common detector for both focal ratios.

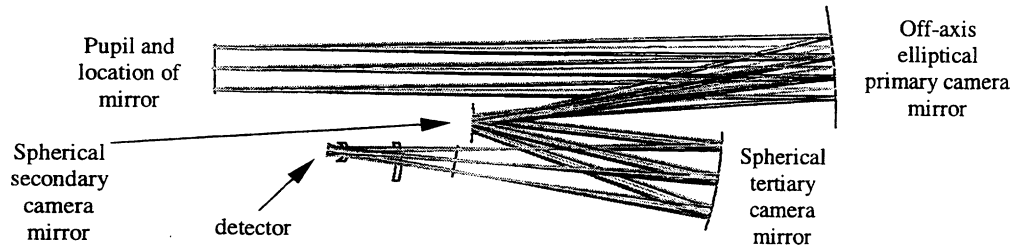

Figure 7. Reflective collimator and camera. A mirror is coincident to the pupil plane on the left and relayed by the reflective three mirror camera for imaging. The two lenses change the focal length of the f/5.6 all reflective camera to f/10.3. The collimating parabola lies beneath the ellipse and is not displayed in the figure.

4.7. High-Resolution spectroscopy

High resolution spectroscopy is an integral part of the instrument. For high resolution and wide spectral coverage, the reflective camera channel is utilized. After the collimating off-axis parabola and two inches before the relayed pupil, a mirror rotates and directs the light to four various directions, 90 degrees apart. The nominal position directs the light to a flat mirror located at the pupil, thus allowing direct imaging of the sky. The other three positions direct the light towards three different gratings.

For highest resolving power, a prism cross-dispersed Echelle grating is used for dispersing a 0.2 arcsecond wide slit for a resolution of 30,000. This mode of spectroscopy is illustrated in Figure 8 and the focal plane shown in Figure 9. For nights with exceptional seeing the same spectrograph can be used with the 0.1 arcsecond slit and the f/10.3 lenses for a resolution of nearly 60,000. The second and third spectrographs use a first order diffraction grating for resolutions above 3,000. The first grating is for the J, H and K windows with an effective resolution of 4,500 while the other grating is for the L and M windows simultaneously. These lower resolution spectrographs have not been finalized.

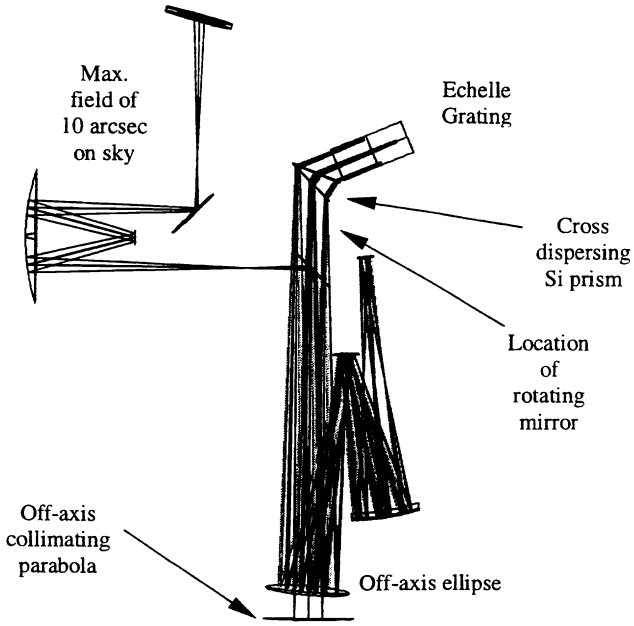

Figure 8. High-order spectroscopy. On-axis light is collimated at the parabola, cross-dispersed at the prism and diffracted at the Echelle grating for a resolution of 30,000 over the 1 to 5 μm spectral region. The rotating mirror is not shown in this figure but its location is indicated.

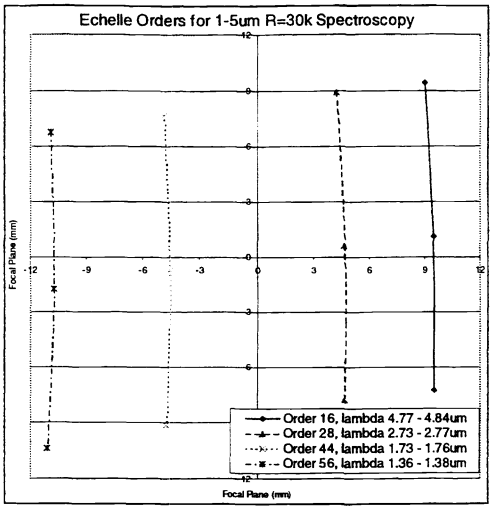

Figure 9. Echelle image plane format. Schematic of Echelle spectral orders superimposed onto the infrared detector for simultaneous J through M band spectroscopy. A slight transmission loss at the lower spectral region is expected due to the cross dispersing Silicon prism. The grating will be slightly tilted to redirect the full wavelength range onto the 18.9mm x 18.9mm detector.

5.EXPECTED SYSTEM PERFORMANCE

Preliminary tolerancing indicated that a series of compensators, optical adjustments after fabrication, would be necessary to ease fabrication and alignment requirements. We planned an alignment procedure for ARIES that would take place in steps and the tolerancing analysis of the optical elements and their physical locations was modeled following this alignment procedure.

One of the prerequisites of the tolerancing analysis was to create a simple methodology to compare the expected performance of the various cameras and spectrographs over the various fields, wavelengths, optical subsystems and detector positions. The method chosen for this task was to evaluate the rms wavefront contribution for manufacturing and alignment errors for each camera and spectrograph subsystem. Additionally, the tolerancing was done at the central wavelength of the optical subsystem and over four field positions: on axis, the $7/10^{th}$ zone, edge of the field and the corner of the field. Each of these optical subsystems was compared to the expected imagery of the best case adaptive optic atmospheric compensation. This AO performance calculation includes the major error sources of fitting error, servo lag, focus anisotropy and tilt anisotropy. (Source magnitude, noise and other sources of error were not considered and it is estimated that the actual performance will be degraded from the comparison values no greater than 20%.) In Figure 10, graphs illustrate the expected performance of the ARIES major optical cameras.

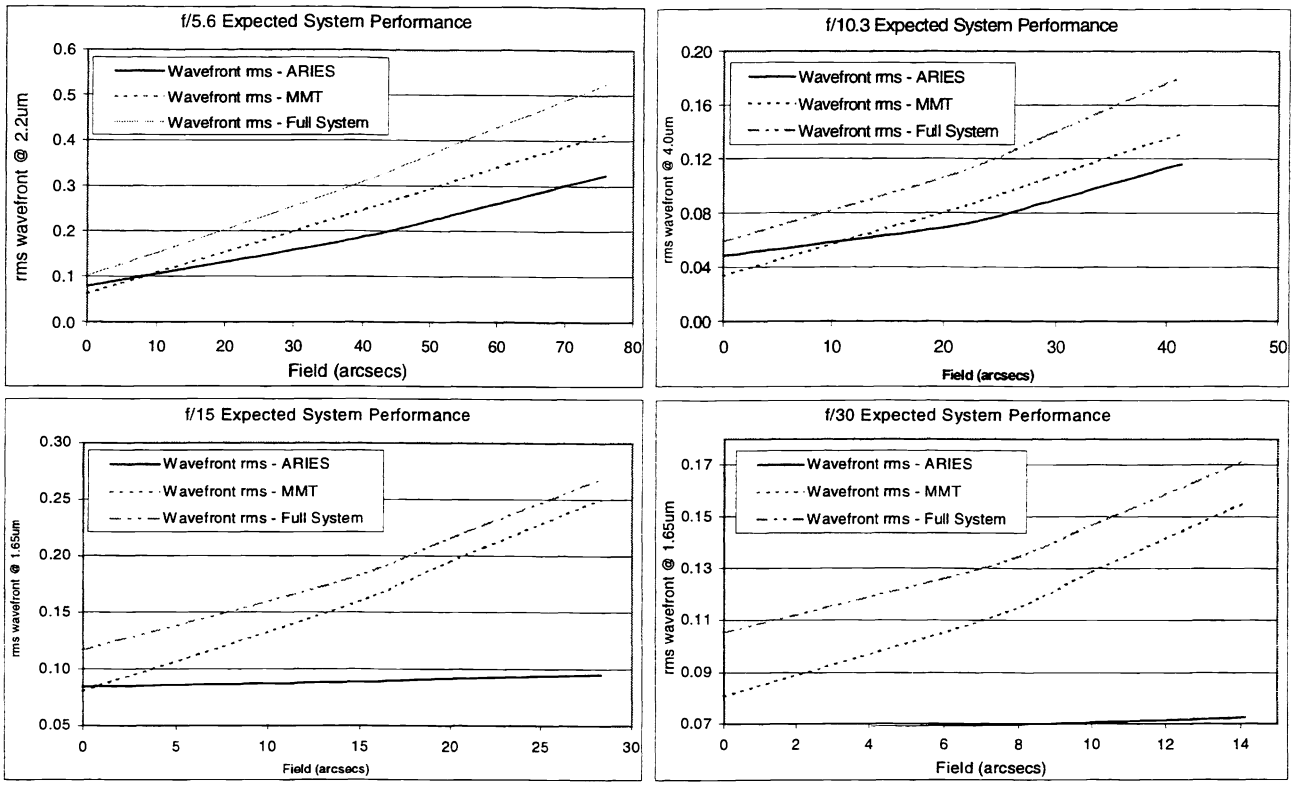

Figure 10. Expected system performance analysis. The graphs compare each of the four cameras in the instrument rms wavefront at the central wavelength to its field. In addition, the graph illustrates the wavefront contribution and graphs the whether the source is from the telescope or instrument. The MMT data includes the primary and secondary telescope mirrors with an adaptive optic system operating at 0.1 arcseconds, the 10% best seeing capability.

From the above expected system performance results in figure 10, if the optical components can be manufactured and aligned within the tolerances specified, in nearly all cases the adaptive optics will be the limiting element of the science cameras. Requirements on most components are relatively relaxed considering an instrument of this caliber. However, some components, the mirrors in particular, required sagitta measurements from nominal to be less than 1.0 μm. For these and similarly difficult components, we have required the final optic to be measured with a known accuracy so that the delivered optical component position can be reoptimized in the ray trace program. This final optical position will be relayed to the opto-mechanical team for final positioning.

Based on the optical materials and various instrument choices, initial calculations show that the throughput of the refractive cameras is approximately 28% with the largest light loss from the detector with 60% efficiency. The two reflective cameras have a higher throughput of nearly 50% with the high order Echelle spectrometer transmitting 36% of the original signal. The calculations include all surfaces in the instrument through the detectors and are based on expected coating performance.

Ghost image analysis was examined for the last two lenses of each refractive camera. The analysis consisted of manually propagating a single reflection of the airy disk diameter at the central wavelength of each camera at the focal plane towards the source and reflecting back off of each lens surface towards the focal plane. The irradiance of the ghost image to the airy disk was negligible for all cases. No stray light analysis was performed.

6. INSTRUMENT STATUS

The instrument is presently in the early phases of component manufacturing with the optical and mechanical design phase complete except for some diffraction analysis and guide star designs. Formal bidding is nearly finished and we completed detailed cost estimations to complete the project. The cryo-mechanical studies are fully developed and detailed element drawings have commenced. The first optical components, the atmospheric dispersion lenses and prisms, are being polished by Optical Solutions Inc. in New Hampshire.

ACKNOWLEDGEMENTS

The authors would like to acknowledge the invaluable assistance of the cryo-mechanical specialists Robert F. Kurtz and Elliott Solheid at Infrared Laboratories, Tucson, AZ. Not only have they shared their invaluable expertise for this project, but after many years of deserving retirement, Bob has repeatedly traded the golf course for our meetings. Bob, we promise we won't add any more accessories!

We have been supported by the National Science Foundation under grant AST 96-23788 and the Air Force Office of Scientific Research under grant #F49620-94-1-0437 and #F49620-96-1-0366.

REFERENCES

[1] J.C. Shelton, M. Lloyd-Hart, J.R.P. Angel and D.G. Sandler, "The 6.5m MMT laser-guided adaptive optics system: Overview and progress report II," Proc. SPIE **3126**, p. 2, 1997.

[2] Ge, Jian, "Sodium laser guide star technique, spectroscopy and imaging with adaptive optics", University of Arizona Astronomy dissertation, 1998.

[3] D.W. McCarthy, J.H. Burge, J.R.P. Angel, J. Ge, R.J. Sarlot, B.C. Fitz-Patrick, and J.L. Hinz, "ARIES: Arizona infrared imager and echelle spectrograph," Proc. SPIE **3354**, p.750, 1998.

[4] Wilson, R. N., *Reflecting telescope optics I*, Springer, Berlin, 1996.

[5] Su, D., -q., 1986, "Astronomical Astrophysics", 156, p.381.

[6] Cook, Lacy, G., "Three mirror anastigmatic optical system", US patent 4,265,510, 1981.